Sequential recognition of discrete export signals in flagellar subunits during bacterial Type III secretion

Authors

Owain J. Bryant[a] , Paraminder Dhillon[a], Colin Hughes[a], Gillian M. Fraser[a,*]

Affiliations

[a]Department of Pathology, University of Cambridge, Tennis Court Road, Cambridge, CB2 1QP, United Kingdom

Corresponding author

[*]Gillian M. Fraser

Department of Pathology, University of Cambridge, Tennis Court Road, Cambridge, CB2 1QP, United Kingdom

Phone: +44 1223 330245

Email: gmf25@cam.ac.uk

Keywords

Type III secretion system; protein export; bacterial flagella biogenesis

[b]Owain Bryant current address: Department of Biochemistry, University of Oxford, South Parks Road, Oxford, OX1 3QU

[c]Paraminder Dhillon current address: The FEBS Journal Editorial Office, 59 St Andrew's House, Cambridge, CB2 3BZ, United Kingdom

Abstract

The flagellar T3SS delivers proteins from the bacterial cytosol to nascent cell surface flagella. Early subunits of the flagellar rod and hook are unchaperoned and contain their own export signals. One export signal, the gate recognition motif (GRM) docks subunits at the export gate, which must then open for unfolded subunits to enter the flagellar channel. Here, we identify a second signal at the extreme N-terminus of flagellar rod/hook subunits and determine that key to the signal is its hydrophobicity. We show that the two export signals are recognised sequentially, with the N-terminal signal being recognised only after subunits have docked at the export gate. The position of the N-terminal signal relative to the GRM is important, as a FlgD deletion variant (FlgDshort), in which the distance between the N-terminal signal and the GRM was shortened, stalled at the export machinery and was not exported. The attenuation of motility caused by FlgDshort was suppressed by mutations that destabilised the closed conformation of the FlhAB-FliPQR flagellar export gate, suggesting that the hydrophobic N-terminal signal might trigger gate opening.

Introduction

Type III Secretion Systems (T3SS) are multi-component molecular machines that deliver protein cargo from the bacterial cytosol either to their site of assembly in cell surface flagella or virulence factor injectosomes, or directly to their site of action in eukaryotic target cells or the extracellular environment [1-5]. The flagellar T3SS (fT3SS) directs the export of thousands of structural subunits required for the assembly and operation of flagella, rotary nanomotors for cell motility that extend from the bacterial cell surface [1],[6]. Newly synthesised subunits of the flagellar rod,

hook and filament are targeted to the fT3SS, where they are unfolded and translocated across the cell membrane, powered by the proton motive force and ATP hydrolysis, into an external export channel that spans the length of the nascent flagellum [7],[8]. During flagellum biogenesis, when the rod/hook structure reaches its mature length, the fT3SS switches export specificity from recognition of 'early' rod/hook subunits to 'late' subunits for filament assembly [9],[10]. This means that early and late flagellar subunits must be differentiated by the fT3SS machinery to ensure that they are exported at the correct stage of flagellum biogenesis. This is achieved, in part, by targeting subunits to the export machinery at the right time using a combination of export signals in the subunit mRNA and/or polypeptide. T3SS substrates contain N-terminal signals for targeting to the export machinery, however these signals do not share a common peptide sequence [11-15]. In addition, some substrates are piloted to the T3SS machinery by specific chaperones [16-21].

The core export components of the fT3SS are evolutionarily related to those of the virulence injectosome, with which they share considerable structural and amino acid sequence similarity [22-25]. The flagellar export machinery comprises an ATPase complex (FliHIJ) located in the cytoplasm, peripheral to the membrane. Immediately above the ATPase is a nonameric ring formed by the cytoplasmic domain of FlhA ($FlhA_C$), which functions as a subunit docking platform [20],[21],[26]. A recent cryo-ET map indicates that the FlhA family have a sea-horse-like structure, in which FlhAc forms the 'body' and the FlhA N-terminal region ($FlhA_N$) forms the 'head', which is fixed in the plane of the membrane [27]. $FlhA_N$ wraps around the base of a complex formed by FliPQR and the N-terminal sub-domain of FlhB ($FlhB_N$), and together

these form the FlhAB-FliPQR export gate that connects the cytoplasm to the central channel in the nascent flagellum, which is contiguous with the extracellular environment [22],[28]. $FlhB_N$ is connected *via* a linker ($FlhB_{CN}$) to the cytoplasmic domain of FlhB ($FlhB_C$), which is thought to sit between the $FlhA_N$ and $FlhA_C$ rings, where it functions as a docking site for early flagellar subunits [22],[14],[28].

The 'early' flagellar subunits that assemble to form the rod and hook substructures are not chaperoned: instead, the signals for targeting and export are found within the early subunits themselves. We have shown that one of these signals is a small hydrophobic sequence termed the gate recognition motif (GRM), which is essential for early subunit export [14]. This motif binds a surface exposed hydrophobic pocket on FlhBc [14]. Once subunits reach the export machinery, they must be unfolded before they can pass through the narrow channel formed by FliPQR-$FlhB_N$ into the central channel of the nascent flagellum, through which the subunits transit until they reach the tip and fold into the structure [22],[6]. Structural studies suggest that FliPQR-$FlhB_N$ adopts an energetically favourable closed conformation, possibly to maintain the membrane permeability barrier [22],[25],[29],[30]. This suggests that there must be a mechanism to trigger opening of the export gate when subunits dock at cytoplasmic face of the flagellar export machinery.

Here we sought to identify new export signals within flagellar rod/hook subunits, using the hook-cap subunit FlgD as a model export substrate. We show that the extreme N-terminus of rod/hook subunits contains a hydrophobic export signal and investigate its functional relationship to the subunit gate recognition motif (GRM).

Results

Identification of a hydrophobic export signal at the N-terminus of FlgD

The N-terminal region of flagellar rod and hook subunits is required for their export [12],[14]. Using the flagellar hook-cap protein FlgD as a model rod/hook subunit, we sought to identify specific export signals within the N-terminus. A screen of ten FlgD variants containing internal five-residue scanning deletions in the first 50 residues (though FlgDΔ2-5 is a four-residue deletion, retaining the initial methionine) identified just two variants defective for export into culture supernatant (**Fig. 1A**). Loss of residues 2-5 caused a significant reduction in export, as did deletion of residues 36-40, though to a lesser extent (**Fig. 1A**; [14]). We have shown that FlgD residues 36-40 are the gate recognition motif (GRM) required for transient subunit docking at the $FlhB_C$ component of the export gate [14]. The results suggest that the extreme N-terminus might also be important for interaction with the export machinery.

To gain insight into the putative new signal, we screened for intragenic suppressor mutations that could restore export of the FlgDΔ2-5 variant. A *Salmonella flgD* null strain expressing *flgD*Δ2-5 *in trans* was inoculated into soft-tryptone agar and incubated until 'spurs' of motile cell populations appeared. Sequencing of *flgD*Δ2-5 alleles from these motile populations identified ten different intragenic gain-of-function mutations. These could be separated into two classes (**Fig. 1B**).

The first class of motile revertants carried *flgD*Δ2-5 alleles with missense mutations that introduced small non-polar residues at the extreme N-terminus of FlgDΔ2-5 (**Fig. 1B**). Deletion of residues 2-5 (^{2}SIAV^{5}) had removed all small non-polar amino acids

from the first ten residue region of FlgD, effectively creating a new N-terminus containing a combination of polar, charged or large non-polar residues (**Fig. S1**). Analysis of other flagellar rod and hook subunit primary sequences revealed that in every case their native N-terminal regions contain small non-polar residues positioned upstream of the gate recognition motif (GRM residues 36-40; **Fig. S1**), indicating that hydrophobicity may be key to the function of the N-terminal export signal. Export assays performed with two representative motile revertant strains carrying *flgDΔ2-5* variants with gain-of-function point mutations, those encoding FlgDΔ2-5-N_8I and FlgDΔ2-5-T_{11}I, revealed that export of these subunits had recovered to ~50% of the level observed for wild type FlgD (**Fig. 1C**; **Fig. S2; Fig. S3**).

The second class of motile revertants carried *flgD*Δ2-5 alleles that had acquired duplications or insertions introducing at least six additional residues between the FlgDΔ2-5 N-terminus and the gate recognition motif (GRM; **Fig. 1B**). It seemed possible that these insertions/duplications might have restored subunit export either by insertion of amino acids that could function as a 'new' hydrophobic export signal, or by restoring the position of an existing small hydrophobic residue or sequence relative to the GRM.

To assess these possibilities, we tested whether export of FlgDΔ2-5 could be recovered by inserting either polar (^{19}STSTST^{20}) or small non-polar (^{19}AGAGAG^{20}) residues in the FlgDΔ2-5 N-terminal region at a position equivalent to one of the suppressing duplications (^{19}GSGSMT^{20}; **Fig. 1B and D**; **Fig. S3**). We reasoned that

if suppression by the additional sequence had been caused by repositioning an existing small hydrophobic amino acid relative to the GRM, then any insertional sequence (polar or non-polar) would restore export, while if suppression had resulted from insertion of a 'new' export signal, then either the polar STSTST or non-polar AGAGAG, but not both, could be expected to restore export.

We found that both the engineered FlgD variants (FlgDΔ2-5-^{19}AGAGAG^{20} and FlgDΔ2-5-^{19}STSTST^{20}) were exported from a *Salmonella flgD* null strain as effectively as the gain-of-function mutant FlgDΔ2-5-^{19}GSGSMT^{20} isolated from the suppressor screen (**Fig. 1D**). This suggests that the insertions had repositioned a sequence in the FlgDΔ2-5 N-terminus relative to the GRM to overcome the loss of small hydrophobic residues.

The position of the hydrophobic export signal relative to the gate recognition motif is critical for rod and hook subunit export

The discovery of intragenic suppressors of the FlgDΔ2-5 export defect indicated that FlgD export requires a hydrophobic signal towards the subunit N-terminus and that the position of this hydrophobic signal relative to the previously described GRM is important. Sequence analysis of the gain-of-function FlgDΔ2-5 insertion variants revealed that the insertions were all located between the GRM and valine$_{15}$ (V$_{15}$; **Fig. 1B**). We reasoned that the insertions repositioned valine$_{15}$ relative to the GRM, such that it could perform the function of the N-terminal hydrophobic signal lost in FlgDΔ2-5. To test this view, we replaced V$_{15}$ with alanine in the gain-of-function variant FlgDΔ2-5-^{19}(GSGSMT)^{20} and assayed its export in the *Salmonella flgD* null (**Fig. 2A**;

Fig. S4). Unlike the *flgD* null strain producing either the parental FlgDΔ2-5-^{19}(GSGSMT)^{20} or wild type FlgD, the *flgD* null carrying variant FlgDΔ2-5-^{19}(GSGSMT)^{20}-V_{15}A was non-motile, reflecting the variant's failure to export (**Fig. 2A**). This suggests that the V_{15} residue had indeed compensated for the missing N-terminal hydrophobic signal.

By screening for intragenic suppressors of the motility defect associated with FlgDΔ2-5-^{19}(GSGSMT)^{20}-V_{15}A, four gain-of-function missense mutations were identified, M_7I, D_9A, T_{11}I and G_{14}V. All of these had introduced small hydrophobic residues, all positioned at least 27 residues upstream of the GRM. These FlgDΔ2-5-^{19}(GSGSMT)^{20}-V_{15}A gain-of-function variants restored motility to the *Salmonella flgD* null strain and were exported at levels similar to wildtype FlgD and FlgDΔ2-5-^{19}(GSGSMT)^{20} (**Fig. 2A**). These data confirm the importance of small non-polar residues positioned upstream of the GRM.

Our results so far had indicated that the position of the FlgD N-terminal hydrophobic export signal relative to the GRM was critical and suggested that, for export to occur efficiently, at least 26 residues must separate the hydrophobic signal and the GRM (**Fig 1C**). In the primary sequences of all *Salmonella* flagellar rod/hook subunits the GRM is positioned ≥ 30 amino acids downstream of the subunit N-terminus (**Fig S1**), suggesting that separation of the two signals by a minimum number of residues might be a common feature among early flagellar subunits. To test this, a suite of engineered *flgD* alleles was constructed that encoded FlgD variants in which wildtype residues 9-32 were replaced with between one and four repeats of the six

amino acid sequence Gly-Ser-Thr-Asn-Ala-Ser (GSTNAS). Swimming motility and export assays revealed that the minimum number of inserted GSTNAS repeats that could support efficient FlgD export was three, equivalent to separation of the hydrophobic N-terminal signal and the GRM by 24 residues (**Fig. 2B**; **Fig. S5**). Below this threshold, FlgD export and swimming motility were strongly attenuated (**Fig. 2B**). A further set of recombinant *flgD* alleles was constructed, which encoded FlgDΔ9-32 variants carrying two GSTNAS repeats (hereafter termed $FlgD_{short}$) directly followed by between one and five additional residues (**Fig. 2C**; **Fig. S5**). Motility and FlgD export increased incrementally with the addition of each amino acid (**Fig. 2C**). The data indicate that a low level of FlgD export is supported when the hydrophobic N-terminal signal ($_{2}SIAV_{5}$) and the GRM ($_{36}FLTLL_{40}$) are separated by 19 residues, with export efficiency and swimming motility increasing as separation of the export signals approaches the optimal 30 residues.

To further establish the requirement for a minimum number of residues between the hydrophobic N-terminal signal and the GRM, we screened for intragenic suppressor mutations that could restore swimming motility in a *flgD* null strain producing $FlgD_{short}$. Sequencing of $flgD_{short}$ alleles from motile revertant strains identified 12 gain-of-function mutations that introduced additional residues between the hydrophobic N-terminal signal and the GRM (**Fig. S6**). Swimming motility and FlgD export was assessed for three *flgD* null strains expressing representative $flgD_{short}$ gain-of-function variants and all showed increased FlgD subunit export and swimming motility compared to the *flgD* null expressing $flgD_{short}$ (**Fig. 2D**; **Fig. S6**).

192 The data confirm that the position of the hydrophobic N-terminal signal relative to the
193 GRM is critical for efficient FlgD subunit export.
194
195 To establish that this is a general requirement for the export of other rod and hook
196 subunits, engineered alleles of *flgE* (hook) and *flgG* (rod) were constructed that
197 encoded variants in which FlgE residues 9-32 or FlgG residues 11-35 were either
198 deleted ($FlgE_{short}$ and $FlgG_{short}$) or replaced with four repeats of the sequence
199 GSTNAS (**Fig. 3**; **Fig. S7**). As had been observed for $FlgD_{short}$, export of the
200 $FlgE_{short}$ and $FlgG_{short}$ variants was severely attenuated compared to wild type FlgE
201 and FlgG (**Fig. 3**). Furthermore, insertion of four GSTNAS repeats into $FlgE_{short}$ and
202 $FlgG_{short}$ recovered subunit export to wild type levels, indicating that the minimum
203 separation of the hydrophobic N-terminal signal and the GRM is a feature throughout
204 rod and hook subunits (**Fig. 3**).
205
206 ***Sequential engagement of the subunit GRM and hydrophobic N-terminal***
207 ***export signal by the flagellar export machinery***
208 Having identified a new hydrophobic N-terminal export signal and established that its
209 position relative to the GRM was critical, we next wanted to determine the order in
210 which the signals were recognised/engaged by the export machinery. The signals
211 might be recognised simultaneously, with both being required for initial entry of
212 rod/hook subunits into the export pathway. Alternatively, they might be recognised
213 sequentially. If this were the case, then a subunit variant that possessed the 'first'
214 signal but was deleted for the 'second' signal might enter the export pathway but fail
215 to progress, becoming stalled at a specific step to block the pathway and prevent

export of wild type subunits. To test if FlgDΔ2-5 or FlgDΔGRM stalled in the export pathway, recombinant expression vectors encoding these variants or wild type FlgD were introduced into a *Salmonella* Δ*recA* strain that is wild type for flagellar export (**Fig. 4**). We could then assess whether the variant FlgD constructs could interfere *in trans* with the wild type flagellar export. We saw that FlgDΔ2-5 inhibited motility and export of the FliK and FlgK flagellar subunits, whereas FlgDΔGRM did not (**Fig. 4B and C**). The data indicate that FlgDΔ2-5 enters the flagellar export pathway and stalls at a critical point, blocking export. In contrast, FlgDΔGRM does not stall or block export.

To determine whether FlgDΔ2-5 stalls at a point before or after subunit docking at the $FlhB_C$ component of the flagellar export gate *via* the GRM, a recombinant vector encoding a FlgD variant in which both export signals were deleted (FlgDΔ2-5ΔGRM) was constructed. If loss of the hydrophobic N-terminal signal had caused subunits to stall after docking at $FlhB_C$, then additional deletion of the subunit GRM would relieve this block. Motility and subunit export assays revealed that the *Salmonella* Δ*recA* strain producing FlgDΔ2-5ΔGRM displayed swimming motility and levels of FliK and FlgK subunit export similar to cells producing FlgDΔGRM (**Fig. 4B and C**). The data suggest that FlgDΔ2-5 stalls after docking at the $FlhB_C$ export gate, preventing docking of other early subunits.

It seemed possible that subunit docking *via* the GRM to the $FlhB_C$ export gate might position the hydrophobic N-terminal signal in close proximity to its recognition site on the export machinery. If this were the case, 'short' subunit variants containing

deletions that decreased the number of residues between the hydrophobic N-terminal signal and the GRM might also stall at $FlhB_C$, and this stalling might be relieved by additional deletion of the GRM. To test this, recombinant expression vectors encoding 'short' subunit variants ($FlgE_{short}$ or $FlgD_{short}$), 'short' subunit variants additionally deleted for the GRM ($FlgE_{short}\Delta GRM$ or $FlgD_{short}\Delta GRM$) or wild type FlgE or FlgD were introduced into a *Salmonella* Δ*recA* strain (**Fig 5**). Compared to the wild type subunits expressed *in trans*, the 'short' subunits inhibited swimming motility and the export of other flagellar subunits (FliD, FliK, FlgK), whereas $FlgE_{short}\Delta GRM$ and $FlgD_{short}\Delta GRM$ did not (**Fig 5**). Taken together with the data presented in Figure 4, the results indicate that the subunit GRM and the hydrophobic N-terminal signal are recognised sequentially, with subunits first docking at $FlhB_C$ *via* the GRM, which positions the hydrophobic N-terminal signal for subsequent interactions with the export machinery (**Fig 4D**).

Mutations that promote opening of the export gate partially compensate for incorrect positioning of the subunit N-terminal export signal

The accruing data indicated that subunit docking at $FlhB_C$ might correctly position the hydrophobic N-terminal signal for recognition by the export machinery. To model the position of $FlhB_C$ relative to other components of the export machinery, we placed the structures of $FlhB_C$ and the FliPQR-$FlhB_N$ export gate into the tomographic reconstruction of the *Salmonella* SPI-1 type III secretion system (**Fig 6B**; [31]). The model indicated that FliPQR-$FlhB_N$ and the subunit docking site on $FlhB_C$ are separated by a minimum distance of ~78 Å, and that $FlhB_C$ is positioned no more than ~22-45 Å from FlhA (Fig 6A; [27]). Taking FlgD as a model early flagellar

subunit, the distance between the FlgD N-terminal hydrophobic signal and the GRM was found to be in the range of ~45 Å (α-helix) to ~105 Å (unfolded contour length), depending on the predicted structure adopted by the subunit N-terminus (Fig 6A). Based on these estimates, it seemed feasible that the hydrophobic N-terminal signal of a subunit docked at $FlhB_C$ could contact either FlhA or the FliPQR-$FlhB_N$ complex, and that this interaction might trigger opening of the export gate [27],[30],[22]. If this were true, mutations that promote the open conformation of the export gate might compensate for the incorrect positioning of the hydrophobic N-terminal export signal in 'short' rod/hook subunits. One such export gate mutation, FliP-M_{210}A, has been shown to increase ion conductance across the bacterial inner membrane, indicating that this gate variant fails to close efficiently [29].

To test whether the FliP-M_{210}A variant gate could promote export of 'short' subunits, in which the distance between the hydrophobic N-terminal signal and the GRM was reduced, a recombinant expression vector encoding $FlgD_{short}$ was introduced into *Salmonella flgD* null strains in which the *fliP* gene had been replaced with recombinant genes encoding either a functional FliP variant with an internal HA-tag (designated wild type gate) or the equivalent HA-tagged FliP-M_{210}A variant (designated M_{210}A gate; **Fig. 6C**; **Fig. S8**). The swimming motility of these strains was found to be consistently stronger in the strain producing the M_{210}A gate compared to the strain with the wild type gate, with the motility halo of the *fliP*-M210A-Δ*flgD* strain expressing $FlgD_{short}$ having a 50% greater diameter than that of the wild type *fliP*-Δ*flgD* strain expressing $FlgD_{short}$ (**Fig. 6D**). This increase in motility indicated that the defect caused by incorrect positioning of the hydrophobic N-

terminal signal relative to the GRM in $FlgD_{short}$ could indeed be partially compensated by promoting the gate open conformation.

Discussion

T3SS substrates contain N-terminal export signals, though these signals have not been fully defined and how they promote subunit export remains unclear. Here, we characterised a new hydrophobic N-terminal export signal in early flagellar rod/hook subunits and showed that the position of this signal relative to the known subunit gate recognition motif (GRM) is key to export.

Loss of the hydrophobic N-terminal signal in the hook cap subunit FlgD had a stronger negative effect on subunit export than deletion of the GRM that enables subunit docking at $FlhB_C$, suggesting that the hydrophobic N-terminal signal may be required to trigger an essential export step. A suppressor screen showed that the export defect caused by deleting the hydrophobic N-terminal signal could be overcome by mutations that either reintroduced small non-polar amino acids positioned 3-7 residues from the subunit N-terminus (*e.g.* M_7I), or introduced additional residues between V_{15} and the GRM. In such 'gain of function' strains containing insertions, changing V_{15} to alanine abolished subunit export, which was rescued by re-introduction of small non-polar residues close to the N-terminus. These data point to an essential export function for small non-polar residues close to the N-terminus of rod/hook subunits.

It was fortuitous that we chose FlgD as the model for early flagellar subunit. All early subunits contain small hydrophobic residues close to the N-terminus, but FlgD is unique in that only four (I_3, A_4, V_5 and V_{15}) of its first 25 residues are small and non-polar (**Fig. S1**). Indeed, there are only three other small hydrophobic residues between the FlgD N-terminus and the GRM (**Fig. 1**). While deletion of residues 2-5 in FlgD removes the critical hydrophobic N-terminal signal, similar deletions in the N-terminal regions of other rod/hook subunits reposition existing small non-polar residues close to the N-terminus (**Fig. S1**). This is perhaps why previous deletion studies in early flagellar subunits have failed to identify the hydrophobic N-terminal signal [14],[37],[38].

The finding that subunits lacking the hydrophobic N-terminal export signal, but not the GRM, stalled during export suggested that these two signals were recognised by the flagellar export machinery in a specific order. Mutant variants of other flagellar export substrates or export components have been observed to block the export pathway. For example, a FlgN chaperone variant lacking the C-terminal 20 residues stalls at the FliI ATPase [39], while a GST-tagged FliJ binds FlhA but is unable to associate correctly with FliI so blocking wild type FliJ interaction with FlhA [40]. These attenuations can be reversed by further mutations that disrupt the stalling interactions. This was also observed for FlgDΔ2-5. Loss of the hydrophobic N-terminal signal resulted in a dominant-negative effect on motility and flagellar export, but this was abolished by subsequent deletion of the GRM. This indicates that FlgDΔ2-5 stalls in the export pathway at $FlhB_C$, blocking the binding site for early flagellar subunits. These data are consistent with sequential recognition of the two

335 export signals: the GRM first docking subunits at FlhB$_C$, and positioning the
336 hydrophobic N-terminal signal to trigger the next export step.
337
338 The position of the subunit hydrophobic N-terminal export signal relative to the GRM
339 appears critical for export. Engineering of *flgD* to encode variants in which the region
340 between the N-terminus and the GRM was replaced with polypeptide sequences of
341 varying lengths showed that these signals must be separated by a minimum of 19
342 residues for detectable export, with substantial export requiring separation by 30
343 residues (**Fig. 3**). When subunits dock at FlhB$_C$, which is likely situated within or just
344 below the plane of the inner membrane, the hydrophobic N-terminal signal is
345 positioned close to the FlhAB-FliPQR export gate (**Fig. 6B**). Subunits in which the
346 GRM and N-terminal signal are brought closer together stall at FlhB$_C$, suggesting
347 that the hydrophobic N-terminal signal is unable to contact its recognition site on the
348 export machinery (**Figs. 5, 6A and 6B**). In all flagellar rod/hook subunits, the GRM is
349 positioned at least 30 residues from the N-terminus (**Fig. S1**). The physical distance
350 between the two signals will depend on the structure adopted by the subunit N-
351 terminus (**Fig. 6A**). The N-terminal region of flagellar subunits is often unstructured
352 in solution [11-15],[32], and such disorder may be an intrinsic feature of flagellar
353 export signals [11-15],[33],[34], as is typical in other bacterial N-terminal export
354 signals such as those in substrates of the Sec and Tat systems [35],[36].
355 Unstructured signals may facilitate multiple interactions with different binding
356 partners during export, and in the case of export systems that transport unfolded
357 proteins they may aid initial entry of substrates into narrow export channels [35].
358

As yet, nothing is known about the structure of the subunit N-terminal domain upon interaction with the flagellar export machinery. Signal peptides in TAT pathway substrates switch between disordered and α-helical conformations depending on the hydrophobicity of the environment [41]. It therefore seems likely that local environments along the flagellar export pathway will influence the conformation of subunit export signals [42],[22]. In flagellar subunits, if the region between the hydrophobic N-terminal signal and the GRM is unstructured and extended, this would correspond to a polypeptide contour length of approximately 72-105 Å (where the length of one amino acid is ~3.6 Å). If the same region were to fold as an α-helix, its length would be approximately 30-36 Å (where one amino acid rises every ~1.5 Å). Without further structural information on subunit interactions with the flagellar export machinery and the precise position of FlhBC within the machinery, it is difficult to determine precisely where the hydrophobic N-terminal signal contacts the machinery.

We speculate that one function of the subunit hydrophobic N-terminal signal might be to trigger opening of the FlhAB-FliPQR export gate, which rests in an energetically favourable closed conformation to maintain the permeability barrier across the bacterial inner membrane [29],[22],[30],[27]. The atomic resolution structure of FliPQR showed that it contains three gating regions [22]. FliR provides a loop (the R-plug) that sits within the core of the structure. Below this, five copies of FliP each provides three methionine residues that together form a methionine-rich ring under which ionic interactions between FliQ residues hold the base of the structure shut (Q-latch).

383 A recent structure of a substrate trapped within the vT3SS revealed conformational
384 changes within the export gate [43]. These changes include a rearrangement of the
385 M-gate methione residues and folding up of the FliR plug to allow substrate passage.
386 If the function of the subunit hydrophobic N-terminal signal was to trigger opening of
387 this gate, we hypothesised that mutations which destabilised the gate's closed
388 conformation would suppress the motility defect associated with $FlgD_{short}$, in which
389 the distance between the N-terminal signal and the GRM is reduced. Introduction of
390 the FliP-M_{210}A mutation, which partially destabilises the gate's closed state, did
391 indeed partly suppress the $FlgD_{short}$ motility defect. We did not find export gate
392 variants that completely destabilised gate closure, but it may be that such mutations
393 disrupt the membrane permeability barrier [29]. This could also explain why in
394 screens for suppressors of FlgDΔ2-5 or $FlgD_{short}$ we did not isolate mutations in
395 genes encoding export gate components (data not shown).
396
397 The surface-exposed hydrophobic GRM-binding pocket on $FlhB_C$ is well conserved
398 across the T3SS SctU family, to which FlhB belongs [14],[44],[45]. Furthermore, the
399 GRM is conserved in all four injectosome early subunits (SctI, SctF, SctP, OrgC) and
400 is located at least 30 residues away from small hydrophobic residues near the
401 subunit N-terminus. It therefore seems plausible that the 'dual signal' mechanism we
402 propose for early flagellar export operates in all T3SS pathways.
403
404 Based on the genetic and biochemical work presented here, we propose a model of
405 sequential recognition of export signals at the T3SS export machinery. Early
406 substrates engage with the GRM-binding pocket on $FlhB_C$, positioning the subunit N-

terminal hydrophobic signal to contact its recognition site. Given that $FlhB_C$ is positioned directly below the FliPQR-$FlhB_N$ gate, the N-terminal hydrophobic signal of substrates docked at $FlhB_C$ would be suitably positioned to trigger export gate opening. Based on the location of $FlhB_C$ and the relative position between export signals, the N-terminal hydrophobic signal could trigger gate opening by indirect interactions with FlhA/FlhB or *via* direct interactions with the FliPQR-$FlhB_N$ export gate components.

In many other pathways, the presence of a substrate triggers opening or assembly of the export channel. The outer membrane chitin transporter in *Vibrio* adopts a closed conformation in which the N-terminus of a neighbouring subunit acts as a pore plug [46]. Chitin binding to the transporter ejects the plug, opening the transport channel and allowing chitin transport [45]. In the Sec pathway, interactions of SecA, ribosomes or pre-proteins with SecYEG can induce conformational changes that promote channel opening [47-49],[35]. In the TAT system, which transports folded substrates across the cytoplasmic membrane, substrate binding to the TatBC complex triggers association with, and subsequent polymerisation of, TatA, which is required for substrate translocation [50],[36]. All of these mechanisms serve both to conserve energy and prevent disruption of the membrane permeability barrier. Our data suggest that in a comparable way the signal of non-polar residues within the N-termini of early rod/hook subunits trigger export gate opening.

Methods

Bacterial strains, plasmids and growth conditions

Salmonella strains and plasmids used in this study are listed in **Supplementary Table 1**. The Δ*flgD*::K_m^R strain in which the *flgD* gene was replaced by a kanamycin resistance cassette was constructed using the λ Red recombinase system [58]. Strains containing chromosomally encoded FliP variants were constructed by aph-I-SceI Kanamycin resistance cassette replacement using pWRG730 [59]. Recombinant proteins were expressed in *Salmonella* from the isopropyl β-D-thiogalactoside-inducible (IPTG) inducible plasmid pTrc99a [60]. Bacteria were cultured at 30–37 °C in Luria-Bertani (LB) broth containing ampicillin (100 μg/ml).

Flagellar subunit export assay

Salmonella strains were cultured at 37 °C in LB broth containing ampicillin and IPTG to mid-log phase (OD_{600nm} 0.6-0.8). Cells were centrifuged (6000*g*, 3 min) and resuspended in fresh media and grown for a further 60 min at 37 °C. The cells were pelleted by centrifugation (16,000*g*, 5 min) and the supernatant passed through a 0.2 μm nitrocellulose filter. Proteins were precipitated with 10% trichloroacetic acid (TCA) and 1% Triton-X100 on ice for 1 hour, pelleted by centrifugation (16,000*g*, 10 min), washed with ice-cold acetone and resuspended in SDS-PAGE loading buffer (volumes calibrated according to cell densities). Fractions were analysed by immunoblotting.

452 **Motility assays**

453 For swimming motility, cultures were grown in LB broth to A600nm 1. Two microliters
454 of culture were inoculated into soft tryptone agar (0.3% agar, 10 g/L tryptone, 5g/L
455 NaCl) containing ampicillin (100 µg/ml). Plates were incubated at 37 °C for between
456 4 and 6 hours unless otherwise stated.

457

458 **Isolation of motile strains carrying suppressor mutations**

459 Cells of the *Salmonella flgD* null strain transformed with plasmids expressing FlgD
460 variants (FlgDΔ2-5, FlgDΔ2-5-^{19}GSGSMT^{20}-V15A or FlgD$_{short}$) were cultured at 37
461 °C in LB broth containing ampicillin (100 µg/ml) to mid-log phase and inoculated into
462 soft tryptone agar (0.3% agar, 10 g/L tryptone, 5g/L NaCl) containing ampicillin (100
463 µg/ml). Plates were incubated at 30 °C until motile 'spurs' appeared. Cells from the
464 spurs were streaked to single colony and cultured to isolate the *flgD* encoding
465 plasmid. Plasmids were transformed into the *Salmonella flgD* null strain to assess
466 whether the plasmids were responsible for the motile suppressor phenotypes.
467 Plasmids were sequenced to identify the suppressor mutations.

468

469 **Quantification and statistical analysis**

470 Experiments were performed at least three times. Immunoblots were quantified using
471 Image Studio Lite. The unpaired two-tailed Student's *t*-test was used to determine *p*-
472 values and significance was determined as $*p < 0.05$. Data are represented as mean
473 ± standard error of the mean (SEM), unless otherwise specified and reported as
474 biological replicates.

475

476 **Author contributions**

477 **Owain J. Bryant**: Conceptualization, Data curation, Investigation, Formal analysis,
478 Methodology, Visualisation, Writing – original draft, Writing – review & editing.
479 **Paraminder Dhillon**: Conceptualization, Data curation, Investigation, Formal
480 analysis, Methodology, Visualisation, Writing – review & editing. **Colin Hughes**:
481 Conceptualization, Data curation, Formal analysis, Funding acquisition,
482 Investigation, Methodology, Project administration, Resources, Supervision,
483 Visualisation, Writing – review & editing. **Gillian M. Fraser**: Conceptualization, Data
484 curation, Formal analysis, Funding acquisition, Investigation, Methodology, Project
485 administration, Resources, Supervision, Visualisation, Writing – original draft, Writing
486 – review & editing.

487

488 **Competing interests**

489 The authors declare no competing interests.

490

491 **Acknowledgements**

492 This work was funded by grants from the Biotechnology and Biological Sciences
493 Research Council (BB/M007197/1) to G.M.F, the Wellcome Trust (082895/Z/07/Z) to
494 C.H. and G.M.F., a Biotechnology and Biological Sciences Research Council
495 studentship to P.D., and a University of Cambridge John Lucas Walker studentship
496 to O.J.B.

497

498 **Materials & Correspondence**

499 Materials are available from the corresponding author upon request.

References

[1] L. D. B. Evans, C. Hughes, and G. M. Fraser, "Building a flagellum in biological outer space.," *Microb. cell (Graz, Austria)*, 2014.

[2] W. Deng *et al.*, "Assembly, structure, function and regulation of type III secretion systems," *Nature Reviews Microbiology*. 2017.

[3] D. Büttner and S. Y. He, "Type III protein secretion in plant pathogenic bacteria," *Plant Physiol.*, 2009.

[4] M. E. Konkel *et al.*, "Secretion of virulence proteins from Campylobacter jejuni is dependent on a functional flagellar export apparatus," *J. Bacteriol.*, 2004.

[5] M. Dongre *et al.*, "Flagella-mediated secretion of a novel Vibrio cholerae cytotoxin affecting both vertebrate and invertebrate hosts," *Commun. Biol.*, 2018.

[6] L. D. B. Evans, C. Hughes, and G. M. Fraser, "Building a flagellum outside the bacterial cell," *Trends in Microbiology*. 2014.

[7] T. Minamino and K. Namba, "Distinct roles of the FliI ATPase and proton motive force in bacterial flagellar protein export," *Nature*, vol. 451, no. 7177, pp. 485–488, 2008.

[8] K. Paul, M. Erhardt, T. Hirano, D. F. Blair, and K. T. Hughes, "Energy source of flagellar type III secretion," *Nature*, 2008.

[9] A. W. Williams, S. Yamaguchi, F. Togashi, S. I. Aizawa, I. Kawagishi, and R. M. Macnab, "Mutations in fliK and flhB affecting flagellar hook and filament assembly in Salmonella typhimurium," *J. Bacteriol.*, 1996.

[10] G. M. Fraser, T. Hirano, H. U. Ferris, L. L. Devgan, M. Kihara, and R. M. Macnab, "Substrate specificity of type III flagellar protein export in Salmonella

is controlled by subdomain interactions in FlhB.," *Mol. Microbiol.*, 2003.

[11] G. Kuwajima, I. Kawagishi, M. Homma, J. Asaka, E. Kondo, and R. M. Macnab, "Export of an N-terminal fragment of Escherichia coli flagellin by a flagellum-specific pathway.," *Proc. Natl. Acad. Sci.*, 2006.

[12] T. Minamino and R. M. Macnab, "Components of the Salmonella flagellar export apparatus and classification of export substrates," *J. Bacteriol.*, 1999.

[13] M. G. Kornacker and A. Newton, "Information essential for cell-cycle-dependent secretion of the 591-residue Caulobacter hook protein is confined to a 21-amino-acid sequence near the N-terminus," *Mol. Microbiol.*, 1994.

[14] L. D. B. Evans, S. Poulter, E. M. Terentjev, C. Hughes, and G. M. Fraser, "A chain mechanism for flagellum growth," *Nature*, vol. 504, no. 7479, pp. 287–290, 2013.

[15] B. M. Végh, P. Gál, J. Dobó, P. Závodszky, and F. Vonderviszt, "Localization of the flagellum-specific secretion signal in Salmonella flagellin," *Biochem. Biophys. Res. Commun.*, 2006.

[16] P. Wattiau, B. Bernier, P. Deslée, T. Michiels, and G. R. Cornelis, "Individual chaperones required for Yop secretion by Yersinia," *Proc. Natl. Acad. Sci. U. S. A.*, 1994.

[17] G. M. Fraser, J. C. Q. Bennett, and C. Hughes, "Substrate-specific binding of hook-associated proteins by FlgN and FliT, putative chaperones for flagellum assembly," *Mol. Microbiol.*, vol. 32, no. 3, pp. 569–580, 1999.

[18] J. Thomas, G. P. Stafford, and C. Hughes, "Docking of cytosolic chaperone-substrate complexes at the membrane ATPase during flagellar type III protein export.," *Proc. Natl. Acad. Sci. U. S. A.*, vol. 101, no. 11, pp. 3945–3950, 2004.

548 [19] Y. Akeda and J. E. Galán, “Chaperone release and unfolding of substrates in
549 type III secretion,” *Nature*, 2005.
550 [20] G. Bange, N. Kümmerer, C. Engel, G. Bozkurt, K. Wild, and I. Sinning, “FlhA
551 provides the adaptor for coordinated delivery of late flagella building blocks to
552 the type III secretion system.,” *Proc. Natl. Acad. Sci. U. S. A.*, vol. 107, no. 25,
553 pp. 11295–11300, 2010.
554 [21] M. Kinoshita, N. Hara, K. Imada, K. Namba, and T. Minamino, “Interactions of
555 bacterial flagellar chaperone-substrate complexes with FlhA contribute to co-
556 ordinating assembly of the flagellar filament,” *Mol. Microbiol.*, vol. 90, no. 6, pp.
557 1249–1261, 2013.
558 [22] L. Kuhlen *et al.*, “Structure of the core of the type iii secretion system export
559 apparatus,” *Nat. Struct. Mol. Biol.*, 2018.
560 [23] P. Abrusci *et al.*, “Architecture of the major component of the type III secretion
561 system export apparatus,” *Nat. Struct. Mol. Biol.*, vol. 20, no. 1, pp. 99–104,
562 2012.
563 [24] K. Eichelberg, C. C. Ginocchio, and J. E. Galan, “Molecular and functional
564 characterization of the Salmonella typhimurium invasion genes invB and invC:
565 Homology of InvC to the F0F1 ATPase family of proteins,” *J. Bacteriol.*, 1994.
566 [25] S. Johnson, L. Kuhlen, J. C. Deme, P. Abrusci, and S. M. Lea, “The Structure
567 of an Injectisome Export Gate Demonstrates Conservation of Architecture in
568 the Core Export Gate between Flagellar and Virulence Type III Secretion
569 Systems,” *MBio*, 2019.
570 [26] Q. Xing, K. Shi, A. Portaliou, P. Rossi, A. Economou, and C. G. Kalodimos,
571 “Structures of chaperone-substrate complexes docked onto the export gate in

572 a type III secretion system," *Nat. Commun.*, 2018.
573 [27] C. Butan, M. Lara-Tejero, W. Li, J. Liu, and J. E. Galán, "High-resolution view
574 of the type III secretion export apparatus in situ reveals membrane remodeling
575 and a secretion pathway.," *Proc. Natl. Acad. Sci. U. S. A.*, 2019.
576 [28] S. Mizuno, H. Amida, N. Kobayashi, S. I. Aizawa, and S. I. Tate, "The NMR
577 structure of FliK, the trigger for the switch of substrate specificity in the flagellar
578 type III secretion apparatus," *J. Mol. Biol.*, 2011.
579 [29] E. Ward, T. T. Renault, E. A. Kim, M. Erhardt, K. T. Hughes, and D. F. Blair,
580 "Type-III secretion pore formed by flagellar protein FliP," *Mol. Microbiol.*, 2018.
581 [30] L. Kuhlen *et al.*, "The substrate specificity switch FlhB assembles onto the
582 export gate to regulate type three secretion," *Nat. Commun.*, 2020.
583 [31] V. A. Meshcheryakov, A. Kitao, H. Matsunami, and F. A. Samatey, "Inhibition
584 of a type III secretion system by the deletion of a short loop in one of its
585 membrane proteins," *Acta Crystallogr. Sect. D Biol. Crystallogr.*, 2013.
586 [32] F. Vonderviszt, R. Ishima, K. Akasaka, and S. I. Aizawa, "Terminal disorder: A
587 common structural feature of the axial proteins of bacterial flagellum?," *J. Mol.*
588 *Biol.*, 1992.
589 [33] C. Weber-Sparenberg *et al.*, "Characterization of the type III export signal of
590 the flagellar hook scaffolding protein FlgD of Escherichia coli," *Arch. Microbiol.*,
591 2006.
592 [34] S. I. Aizawa, F. Vonderviszt, R. Ishima, and K. Akasaka, "Termini of
593 Salmonella flagellin are disordered and become organized upon
594 polymerization into flagellar filament," *J. Mol. Biol.*, 1990.
595 [35] A. Tsirigotaki, J. De Geyter, N. Šoštarić, A. Economou, and S. Karamanou,

"Protein export through the bacterial Sec pathway," *Nature Reviews Microbiology*. 2017.

[36] T. Palmer and B. C. Berks, "The twin-arginine translocation (Tat) protein export pathway," *Nature Reviews Microbiology*. 2012.

[37] T. Hirano, S. Shibata, K. Ohnishi, T. Tani, and S. I. Aizawa, "N-terminal signal region of FliK is dispensable for length control of the flagellar hook," *Mol. Microbiol.*, 2005.

[38] T. Minamino, B. González-Pedrajo, K. Yamaguchi, S. I. Aizawa, and R. M. Macnab, "FliK, the protein responsible for flagellar hook length control in Salmonella, is exported during hook assembly," *Mol. Microbiol.*, 1999.

[39] J. Thomas, G. P. Stafford, and C. Hughes, "Docking of cytosolic chaperone-substrate complexes at the membrane ATPase during flagellar type III protein export," *Proc. Natl. Acad. Sci.*, 2004.

[40] T. Ibuki, Y. Uchida, Y. Hironaka, K. Namba, K. Imada, and T. Minamino, "Interaction between FliJ and FlhA, components of the bacterial flagellar type iii export apparatus," *J. Bacteriol.*, 2013.

[41] M. San Miguel, R. Marrington, P. M. Rodger, A. Rodger, and C. Robinson, "An Escherichia coli twin-arginine signal peptide switches between helical and unstructured conformations depending on the hydrophobicity of the environment," *Eur. J. Biochem.*, 2003.

[42] M. Erhardt *et al.*, "Mechanism of type-III protein secretion: Regulation of FlhA conformation by a functionally critical charged-residue cluster," *Mol. Microbiol.*, vol. 104, no. 2, pp. 234–249, 2017.

[43] S. Miletic, D. Fahrenkamp, N. Goessweiner-Mohr, J. Wald, M. Pantel, O.

Vesper, V. Kotov, and T. Marlovits. "Substrate-engaged type III secretion system structures reveal gating mechanism for unfolded protein translocation" bioRxiv., **doi:** https://doi.org/10.1101/2020.12.17.423328

[44] R. Zarivach *et al.*, “Structural analysis of the essential self-cleaving type III secretion proteins EscU and SpaS,” *Nature*, 2008.

[45] G. T. Lountos, B. P. Austin, S. Nallamsetty, and D. S. Waugh, “Atomic resolution structure of the cytoplasmic domain of Yersinia pestis YscU, a regulatory switch involved in type III secretion,” *Protein Sci.*, 2009.

[46] A. Aunkham *et al.*, “Structural basis for chitin acquisition by marine Vibrio species,” *Nat. Commun.*, 2018.

[47] Y. Ge, A. Draycheva, T. Bornemann, M. V. Rodnina, and W. Wintermeyer, “Lateral opening of the bacterial translocon on ribosome binding and signal peptide insertion,” *Nat. Commun.*, 2014.

[48] J. Zimmer, Y. Nam, and T. A. Rapoport, “Structure of a complex of the ATPase SecA and the protein-translocation channel,” *Nature*, 2008.

[49] R. M. Voorhees, I. S. Fernández, S. H. W. Scheres, and R. S. Hegde, “Structure of the mammalian ribosome-Sec61 complex to 3.4 Å resolution,” *Cell*, 2014.

[50] H. Mori and K. Cline, “A twin arginine signal peptide and the pH gradient trigger reversible assembly of the thylakoid ΔpH/Tat translocase,” *J. Cell Biol.*, 2002.

[51] L. D. B. Evans, P. M. Bergen, O. J. Bryant, and G. M. Fraser, “Interactions of flagellar structural subunits with the membrane export machinery,” in *Methods in Molecular Biology*, 2017.

644 [53] F. H. Login and H. Wolf-Watz, “YscU/FlhB of Yersinia pseudotuberculosis
645 harbors a C-terminal type III secretion signal,” *J. Biol. Chem.*, 2015.
646 [54] S. Frost, O. Ho, F. H. Login, C. F. Weise, H. Wolf-Watz, and M. Wolf-Watz,
647 “Autoproteolysis and Intramolecular Dissociation of Yersinia YscU Precedes
648 Secretion of Its C-Terminal Polypeptide YscUCC,” *PLoS One*, 2012.
649 [55] T. Minamino, Y. V. Morimoto, N. Hara, and K. Namba, “An energy transduction
650 mechanism used in bacterial flagellar type III protein export,” *Nat. Commun.*,
651 2011.
652 [56] M. Baba *et al.*, “Rotation of artificial rotor axles in rotary molecular motors,”
653 *Proc. Natl. Acad. Sci.*, 2016.
654 [57] N. Hara, K. Namba, and T. Minamino, “Genetic characterization of conserved
655 charged residues in the bacterial flagellar type III export protein FlhA,” *PLoS*
656 *One*, vol. 6, no. 7, 2011.
657 [58] K. A. Datsenko and B. L. Wanner, “One-step inactivation of chromosomal
658 genes in Escherichia coli K-12 using PCR products,” *Proc. Natl. Acad. Sci. U.*
659 *S. A.*, 2000.
660 [59] S. Hoffmann, C. Schmidt, S. Walter, J. K. Bender, and R. G. Gerlach,
661 “Scarless deletion of up to seven methylaccepting chemotaxis genes with an
662 optimized method highlights key function of CheM in Salmonella
663 Typhimurium,” *PLoS One*, 2017.
664 [60] E. Amann, B. Ochs, and K. J. Abel, “Tightly regulated tac promoter vectors
665 useful for the expression of unfused and fused proteins in Escherichia coli,”
666 *Gene*, 1988.
667 [61] B. Hu, M. Lara-Tejero, Q. Kong, J. E. Galán, and J. Liu, “In Situ Molecular

668 Architecture of the Salmonella Type III Secretion Machine," *Cell*, 2017.

669 [62] T. Minamino and R. M. Macnab, "Domain structure of Salmonella FlhB, a

670 flagellar export component responsible for substrate specificity switching," *J.*

671 *Bacteriol.*, 2000.

672 [63] J. Kyte and R. F Doolittle, "A simple method for displaying the hydropathic

673 character of a protein". *J. Mol. Biol.*, 1982.

674

675

676

677 **Figure legends**

678 **Figure 1. Screening for export-defective FlgD variants**

679 **a.** Whole cell (cell) and supernatant (sec) proteins from late exponential phase
680 cultures of a *Salmonella flgD* null strain expressing wild type FlgD (FlgD) or its
681 variants (Δ2-5, Δ6-10, Δ11-15, Δ16-20, Δ21-25, Δ26-30, Δ31-35, Δ36-40, Δ41-45 or
682 Δ46-50) were separated by SDS (15%)-PAGE and analysed by immunoblotting with
683 anti-FlgD polyclonal antisera.

684 **b.** A schematic displaying the intragenic suppressor mutations within amino acids 1-
685 40 of FlgD isolated from the FlgDΔ2-5 variant. Small non-polar residues are
686 highlighted in orange. All suppressor mutations were located between the gate-
687 recognition motif (GRM, blue) and the extreme N-terminus, and can be separated
688 into two classes: insertions or duplications that introduced additional sequence
689 between valine-15 and the gate-recognition motif, or missense mutations that re-
690 introduce small non-polar residues at the N-terminus.

691 **c**. Whole cell (cell) and supernatant (sec) proteins from late exponential-phase
692 cultures of *Salmonella flgD* null strains expressing suppressor mutants isolated from
693 the FlgDΔ2-5 variant (FlgDΔ2-5-N_8I or FlgDΔ2-5-T_{11}I), FlgDΔ2-5 variant (-) or wild
694 type FlgD (FlgD) were separated by SDS (15%)-PAGE and analysed by
695 immunoblotting with anti-FlgD polyclonal antisera.

696 **d.** Whole cell (cell) and supernatant (sec) proteins from late exponential phase
697 cultures of *Salmonella flgD* null strains expressing wild type FlgD (FlgD), FlgDΔ2-5
698 (DΔ2-5) or variants of FlgDΔ2-5 containing between residues 19 and 20 a six-
699 residue insertion of either small non-polar (AGAGAG) residues (3x(AG)), polar

(STSTST) residues (3x(ST)), or the sequence from an isolated insertion suppressor mutant (GSGSMT), were separated by SDS (15%)-PAGE and analysed by immunoblotting with anti-FlgD polyclonal antisera.

Figure 2. Export of FlgD variants in which the position of the N-terminal hydrophobic export signal is varied relative to the gate recognition motif (GRM)

Whole cell (cell) and supernatant (sec) proteins from late exponential-phase cultures of a *Salmonella flgD* null strain expressing suppressor mutants isolated from the FlgDΔ2-5-^{19}(GSGSMT)^{20}-$V_{15}A$ variant ($V_{15}A$-M_7I, $V_{15}A$-D_9A, $V_{15}A$-$T_{11}I$, $V_{15}A$-$G_{14}V$), their parent FlgD variant FlgDΔ2-5-^{19}(GSGSMT)^{20}-$V_{15}A$ (labelled as $V_{15}A$), FlgDΔ2-5-^{19}(GSGSMT)^{20} (labelled as -) or wild type FlgD (FlgD) were separated by SDS (15%)-PAGE and analysed by immunoblotting with anti-FlgD polyclonal antisera. Swimming motility (bottom panel; 0.25% soft tryptone agar) of the same strains was assayed at 37ºC for 4-6 hours.

b. Whole cell (cell) and supernatant (sec) proteins from late exponential-phase cultures of a *Salmonella flgD* null strain expressing wild type FlgD (FlgD), FlgDΔ9-32 or its variants in which residues 9-32 were replaced by between one and four six-residue repeats of Gly-Ser-Thr-Asn-Ala-Ser (Δ9-32 4xRpt, Δ9-32 3xRpt, Δ9-32 2xRpt or Δ9-32 1xRpt) were separated by SDS (15%)-PAGE and analysed by immunoblotting with anti-FlgD polyclonal antisera. Swimming motility (bottom panel; 0.25% soft tryptone agar) of the same strains was assayed at 37ºC for 4-6 hours.

c. Whole cell (cell) and supernatant (sec) proteins from late exponential-phase cultures of a *Salmonella flgD* null strain expressing wild type FlgD (FlgD), a FlgD variant in which residues 9-32 were replaced by two repeats of a six-residue sequence Gly-Ser-Thr-Asn-Ala-Ser (labelled as 2xRpt) or its variants containing between one and five additional residues inserted directly after the two repeats (2xRpt+1, 2xRpt+2, 2xRpt+3, 2xRpt+4 or 2xRpt+5) were separated by SDS (15%)-PAGE and analysed by immunoblotting with anti-FlgD polyclonal antisera. Swimming motility (bottom panel; 0.25% soft tryptone agar) of the same strains was assayed at 37ºC for 4-6 hours.

d. Whole cell (cell) and supernatant (sec) proteins from late exponential-phase cultures of a *Salmonella flgD* null strain expressing wild type FlgD (FlgD), a FlgD variant in which residues 9-32 were replaced by two repeats of a six-residue sequence Gly-Ser-Thr-Asn-Ala-Ser ($FlgD_{short}$) or suppressor mutants isolated from this strain (rev1, rev2 or rev3) were separated by SDS (15%)-PAGE and analysed by immunoblotting with anti-FlgD polyclonal antisera. Swimming motility (bottom panel; 0.25% soft tryptone agar) of the same strains were was assayed at 37ºC for 4-6 hours.

e. N-terminal sequences of wild type FlgD, a FlgD variant in which residues 9-32 are replaced by two repeats of a six-residue sequence Gly-Ser-Thr-Asn-Ala-Ser (yellow; $FlgD_{short}$) and its suppressor mutant revertants (rev 1-3) aligned at the gate recognition motif (GRM, blue). Suppressor mutants contained insertions (underlined) that introduced additional residues between the N-terminal hydrophobic signal (orange) and the gate recognition motif (blue).

Figure 3. Effect of the relative position of the N-terminus and GRM on the export of rod and hook subunits

a. Schematic representation of a wild type subunit ($subunit_{wild\ type}$), a subunit containing a deletion of sequence between the N-terminus and GRM ($subunit_{short}$) and a subunit in which the deleted sequence was replaced by four repeats of a six-residue sequence Gly-Ser-Thr-Asn-Ala-Ser (yellow, $subunit_{short}$+4Rpt).

b. Whole cell (cell) and supernatant (sec) proteins from late exponential-phase cultures of a *Salmonella flgE* null strain expressing wild type FlgG ($FlgG_{wild\ type}$), a FlgG variant in which residues 11-35 were deleted ($FlgG_{short}$) or a FlgG variant in which residues 11-35 were replaced by four repeats of a six-residue sequence Gly-Ser-Thr-Asn-Ala-Ser ($FlgG_{short}$+4Rpt). All FlgG variants were engineered to contain an internal 3xFLAG tag for immunodetection. Proteins were separated by SDS (15%)-PAGE and analysed by immunoblotting with anti-FLAG monoclonal antisera. Swimming motility (bottom panel; 0.25% soft tryptone agar) of the same strains was assayed at 37ºC for 4-6 hours.

c. Whole cell (cell) and supernatant (sec) proteins from late exponential-phase cultures of a *Salmonella flgD* null strain expressing wild type FlgE ($FlgE_{wild\ type}$), a FlgE variant in which residues 9-32 were deleted ($FlgE_{short}$) or a FlgE variant in which residues 9-32 were replaced by four repeats of a six-residue sequence Gly-Ser-Thr-Asn-Ala-Ser ($FlgE_{short}$+4Rpt). All FlgE variants were engineered to contain an internal 3xFLAG tag for immunodetection. Proteins were separated by SDS (15%)-

767 PAGE and analysed by immunoblotting with anti-FLAG monoclonal antisera.
768 Swimming motility (bottom panel; 0.25% soft tryptone agar) of the same strains was
769 assayed at 37ºC for 4-6 hours.

770 **Figure 4. Effect on subunit export of overexpression of FlgDΔ2-5 and variants.**

771 **a.** Schematic representation of a FlgD subunit containing a N-terminal hydrophobic
772 signal (orange, 2-5) and a gate-recognition motif (blue, GRM).

773 **b.** Swimming motility of a *Salmonella* Δ*recA* strain expressing wild type FlgD (FlgD),
774 its variants (DΔ2-5ΔGRM, DΔ2-5 or DΔGRM) or empty pTrc99a vector (-). Motility
775 was assessed in 0.25% soft-tryptone agar containing 100 µg/ml ampicillin and
776 100µM IPTG and incubated for 4-6 hours at 37°C.

777

778 **c.** Whole cell (cell) and secreted proteins (secreted) from late-exponential-phase
779 cultures were separated by SDS (15%)-PAGE and analysed by immunoblotting with
780 anti-FliK, anti-FlgK, anti-FlgL, anti-FlhA or anti-FlgN polyclonal antisera. Apparent
781 molecular weights are in kilodaltons (kDa).

782 **d**. A model depicting a FlgDΔ2-5 subunit (left) docked *via* its gate recognition motif
783 (GRM, blue) at the subunit binding pocket on $FlhB_C$ (PDB: 3B0Z[31], red), preventing
784 wild type subunits (right) from docking at $FlhB_C$.

785

786

Figure 5. Effect on subunit export of overexpressed $FlgE_{short}$, $FlgD_{short}$ and variants

a. Swimming motility of a *Salmonella* Δ*recA* strain expressing wild type FlgE (FlgE wild type), a FlgE variant in which residues 9-32 were deleted ($FlgE_{short}$), a FlgE variant in which residues 9-32 and residues 39-43 (corresponding to the gate-recognition motif) were deleted ($FlgE_{short}$ΔGRM), a FlgE variant in which residues 39-43 were deleted (FlgEΔGRM) or empty pTrc99a vector (-). All FlgG variants were engineered to contain an internal 3xFLAG tag for immunodetection. Motility was assessed in 0.25% soft-tryptone agar containing 100 µg/ml ampicillin and 100 µM IPTG and incubated for 4-6 hours at 37°C (top panel). Whole cell (cell) and secreted proteins (secreted) from late-exponential-phase cultures were separated by SDS (15%)-PAGE and analysed by immunoblotting with anti-FLAG monoclonal antisera or anti-FlgD, anti-FliD, anti-FlgK, anti-FliK, anti-FlhA or anti-FlgN polyclonal antisera (bottom). Apparent molecular weights are in kilodaltons (kDa).

b. Swimming motility of a *Salmonella* Δ*recA* strain expressing wild type FlgD (FlgD wild type), a FlgD variant in which residues 9-32 were replaced with two repeats of the six amino acid sequence Gly-Ser-Thr-Asn-Ala-Ser ($FlgD_{short}$), a FlgD variant in which residues 9-32 were replaced with two repeats of the six amino acid sequence Gly-Ser-Thr-Asn-Ala-Ser and residues 36-40 were deleted ($FlgD_{short}$ΔGRM), a FlgD variant in which residues 36-40 were deleted (FlgDΔGRM) or empty pTrc99a vector (-). Motility was assessed in 0.25% soft-tryptone agar containing 100 µg/ml ampicillin and 100 µM IPTG and incubated for 4-6 hours at 37°C (top panel). Whole cell (cell) and secreted proteins (secreted) from late-exponential-phase cultures were

separated by SDS (15%)-PAGE and analysed by immunoblotting with anti-FlgD, anti-FliD, anti-FlgK, anti-FliK, anti-FlhA or anti-FlgN polyclonal antisera (bottom). Apparent molecular weights are in kilodaltons (kDa).

Figure 6. Suppression of the $FlgD_{short}$ motility defect by mutations in FliP

a. A model depicting subunits docked *via* their gate-recognition motif (GRM, blue) at the subunit binding pocket on $FlhB_C$ (PDB: 3B0Z [31], red) with N-termini of early flagellar subunits adopting either an α-helical conformation separating the N-terminal hydrophobic signal (2-5, orange) and gate-recognition motif (GRM, blue) by ~40-60 Ångstrom (where each amino acid is on average separated by ~1.5Å, left) or an unfolded conformation where the polypeptide contour length separating the N-terminal hydrophobic signal (2-5) and gate-recognition motif (GRM) is ~90-150 Ångstrom (where each amino acid is on average separated by ~3.5Å, middle left). Values corresponding to the distance separating the N-terminal hydrophobic signal (2-5, orange) and gate-recognition motif (GRM, blue) of a FlgD subunit variant in which residues 9-32 are replaced with two repeats of the six amino acid sequence Gly-Ser-Thr-Asn-Ala-Ser ($FlgD_{short}$) indicate that the N-terminal hydrophobic signal (2-5, orange) and gate-recognition motif (GRM, blue) are separated by ~29 Ångstrom (α-helical conformation, middle right) or ~67 Ångstrom (unfolded polypeptide contour length, right).

b. Placement of the crystal structure of FlhBc (PDB:3BOZ [31]; red) and the cryo-EM structure of FliPQR-FlhB (PDB:6S3L[30]) in a tomographic reconstruction of the *Salmonella* SPI-1 injectisome (EMD-8544 [60]; grey). The minimum distance between the subunit gate recognition motif binding site on $FlhB_C$ (grey) to $FlhB_N$

(defined as *Salmonella* FlhB residue 211 [62]; ~78Å) was estimated by combining: the value corresponding to the distance between the subunit binding pocket on $FlhB_C$ [14] (grey) and the N-terminal visible residue (D_{229}) in the $FlhB_C$ structure (PDB:3BOZ [31]; ~52Å) with the value corresponding to the minimum distance between FlhB residues 211 and 228 (based on a linear α-helical conformation; ~26Å).

c. Swimming motility of recombinant *Salmonella flgD* null strains producing a chromosomally-encoded FliP-$M_{210}A$ variant ($M_{210}A$ gate, left) or wild type FliP (wild type gate, right). Wild type FliP and FliP-$M_{210}A$ were engineered to contain an internal HA tag positioned between residue 21 and 22 to allow immunodetection of FliP. Both strains produced either a pTrc99a plasmid-encoded FlgD subunit variant in which residues 9-32 were replaced with two repeats of the six amino acid sequence Gly-Ser-Thr-Asn-Ala-Ser ($FlgD_{short}$; top panel) or a pTrc99a plasmid-encoded wild type FlgD subunit ($FlgD_{wild\ type}$; bottom panel). Motility was assessed in 0.25% soft-tryptone agar containing 100 µg/ml ampicillin and 50 µM IPTG and incubated for 16 hours (top panel) or 4-6 hours at 37°C (bottom panel).

d. The mean motility halo diameter of a recombinant *Salmonella flgD* null strain producing chromosomally-encoded FliP-$M_{210}A$ ($M_{210}A$ gate, left) and expressing the FlgD short variant (left hand bar) was plotted as a percentage of the mean motility halo diameter of the wild type FliP gate strain (wild type) producing FlgDshort (right hand bar). Error bars show the standard error of the mean calculated from four biological replicates. * indicates a p-value < 0.05.

Supplementary Figure Legends

Figure S1.

a. N-terminal sequences of all *Salmonella* flagellar rod and hook subunits aligned at their gate recognition motif (GRM, blue). Small non-polar residues upstream of the gate recognition motif are highlighted (yellow).

b. Hydrophobicity plots for the N-terminal 60 residues of each *Salmonella* flagellar rod and hook subunit were generated by ExPASy tools using the Kyte and Doolittle method [62]. The *x* axis of the plot indicates the amino acid position, starting from the N terminus. The *y* axis of the plot indicates the hydrophobicity of the amino acid sequence, where higher values represent higher hydrophobicity. Amino acid sequence corresponding to the gate-recognition motif of each subunit is highlighted in blue.

Figure S2

a. Swimming motility of a *Salmonella* Δ*recA* strain expressing suppressor mutants isolated from the FlgDΔ2-5 variant (FlgDΔ2-5 N_8I or FlgDΔ2-5 T_{11}I), the parent FlgDΔ2-5 variant (DΔ2-5) or wild type FlgD (FlgD). Motility was assessed in 0.25% soft-tryptone agar containing 100 µg/ml ampicillin and 50 µM IPTG and incubated 4-6 hours at 37°C.

b. Swimming motility of a *Salmonella* Δ*recA* strain expressing wild type FlgD (FlgD), FlgDΔ2-5 (DΔ2-5) or its variants containing a six-residue insertion between residues 19 and 20 of either small non-polar (AGAGAG) residues (DΔ2-5 3x(AG)), polar

(STSTST) residues (DΔ2-5 3x(ST)), or the sequence from an isolated insertion suppressor mutant (GSGSMT) (DΔ2-5 GSGSMT). Motility was assessed in 0.25% soft-tryptone agar containing 100 µg/ml ampicillin and 50 µM IPTG and incubated 4-6 hours at 37°C.

Figure S3

a. Whole cell (cell) and supernatant (secreted) proteins from late exponential-phase cultures of *Salmonella flgD* null strains expressing: suppressor mutants isolated from the FlgDΔ2-5 variant (FlgDΔ2-5 N_8I or FlgDΔ2-5 $T_{11}I$), FlgDΔ2-5 variant (-) or wild type FlgD (FlgD) were separated by SDS (15%)-PAGE and analysed by immunoblotting with anti-FlhA or FlgN polyclonal antisera. Apparent molecular weights are in kilodaltons (kDa).

b. Whole cell (cell) and supernatant (secreted) proteins from late exponential-phase cultures of *Salmonella flgD* null strains expressing wild type FlgD (FlgD), FlgDΔ2-5 (DΔ2-5) or its variants containing a six-residue insertion between residues 19 and 20 of either small non-polar (AGAGAG) residues (DΔ2-5 3x(AG)), polar (STSTST) residues (DΔ2-5 3x(ST)), or the sequence from an isolated insertion suppressor mutant (GSGSMT) (DΔ2-5 GSGSMT) were separated by SDS (15%)-PAGE and analysed by immunoblotting with anti-FlgD polyclonal antisera. Apparent molecular weights are in kilodaltons (kDa).

Figure S4

a. Whole cell (cell) and supernatant (secreted) proteins from late exponential-phase cultures of a *Salmonella flgD* null strain expressing suppressor mutants isolated from a FlgDΔ2-5-^{19}(GSGSMT)^{20}-$V_{15}A$ variant ($V_{15}A$-M_7I, $V_{15}A$-D_9A, $V_{15}A$-$T_{11}I$, $V_{15}A$-$G_{14}V$), their parent FlgD variant FlgDΔ2-5-^{19}(GSGSMT)^{20}-$V_{15}A$ ($V_{15}A$), FlgDΔ2-5-^{19}(GSGSMT)^{20} (-) or wild type FlgD (FlgD) were separated by SDS (15%)-PAGE and analysed by immunoblotting with anti-FlhA and FlgN polyclonal antisera. Apparent molecular weights are in kilodaltons (kDa).

Figure S5

a. Whole cell (cell) and supernatant (secreted) proteins from late exponential-phase cultures of a *Salmonella flgD* null strain expressing wild type FlgD (FlgD), FlgDΔ9-32 or its variants in which residues 9-32 were replaced by between one and four six-residue repeats of Gly-Ser-Thr-Asn-Ala-Ser (GSTNAS): (Δ9-32 4xRpt, Δ9-32 3xRpt, Δ9-32 2xRpt, Δ9-32 1xRpt) were separated by SDS (15%)-PAGE and analysed by immunoblotting with anti-FlhA and anti-FlgN polyclonal antisera. Apparent molecular weights are in kilodaltons (kDa).

b. Whole cell (cell) and supernatant (secreted) proteins from late exponential-phase cultures of a *Salmonella flgD* null strain expressing wild type FlgD (FlgD), a FlgD variant in which residues 9-32 were replaced by two repeats of a six-residue sequence Gly-Ser-Thr-Asn-Ala-Ser (2xRpt) or its variants containing between one and five additional residues inserted directly after the two repeats (2xRpt+ 1, 2xRpt+ 2, 2xRpt+ 3, 2xRpt+ 4 or 2xRpt+ 5) were separated by SDS (15%)-PAGE and

928 analysed by immunoblotting with anti-FlgD polyclonal antisera. Apparent molecular
929 weights are in kilodaltons (kDa).
930
931 **Figure S6**
932 **a**. Whole cell (cell) and supernatant (secreted) proteins from late exponential-phase
933 cultures of a *Salmonella flgD* null strain expressing wild type FlgD (FlgD), a FlgD
934 variant in which residues 9-32 were replaced by two repeats of a six-residue
935 sequence Gly-Ser-Thr-Asn-Ala-Ser ($FlgD_{short}$) or suppressor mutants isolated from
936 this strain (rev1, rev2 or rev3) were separated by SDS (15%)-PAGE and analysed by
937 immunoblotting with anti-FlhA and anti-FlgN polyclonal antisera. Apparent molecular
938 weights are in kilodaltons (kDa).
939
940 **b**. N-terminal sequences of wild type FlgD (wild type), a FlgD variant in which residus
941 9-32 are replaced by two repeats of a six-residue sequence Gly-Ser-Thr-Asn-Ala-Ser
942 (yellow; $FlgD_{short}$) and its suppressor mutants (rev 1-7) aligned to their gate-
943 recognition motif (GRM, blue). Suppressor mutants contained insertions (underlined)
944 that introduced additional residues between the N-terminal hydrophobic signal
945 (orange) and the gate-recognition motif (blue).
946
947 **Figure S7**
948 **a**. Whole cell (cell) and supernatant (sec) proteins from late exponential-phase
949 cultures of a *Salmonella flgE* null strain expressing wild type FlgG ($FlgG_{wild\ type}$), a
950 FlgG variant in which residues 11-35 were deleted ($FlgG_{short}$) or a FlgG variant in
951 which residues 11-35 were replaced by four repeats of a six-residue sequence Gly-

Ser-Thr-Asn-Ala-Ser ($FlgG_{short}$+4Rpt). All FlgG variants were engineered to contain an internal 3xFLAG tag for immunodetection. Proteins were separated by SDS (15%)-PAGE and analysed by immunoblotting with anti-FlhA or anti-FlgN polyclonal antisera. Apparent molecular weights are in kilodaltons (kDa).

b. Whole cell (cell) and supernatant (secreted) proteins from late exponential-phase cultures of a *Salmonella flgD* null strain expressing wild type FlgE ($FlgE_{wild\ type}$), a FlgE variant in which residues 9-32 were deleted ($FlgE_{short}$) or a FlgE variant in which residues 9-32 were replaced by four repeats of a six-residue sequence Gly-Ser-Thr-Asn-Ala-Ser ($FlgE_{short}$+4Rpt). All FlgE variants were engineered to contain an internal 3xFLAG tag for immunodetection. Proteins were separated by SDS (15%)-PAGE and analysed by immunoblotting with anti-FLAG monoclonal antisera. Swimming motility (bottom panel; 0.25% soft tryptone agar) of the same strains were carried out at 37ºC for 4-6 hours. Apparent molecular weights are in kilodaltons (kDa).

Figure S8

a. Whole cell (cell) proteins from late exponential-phase cultures of recombinant *Salmonella flgD* null strains producing a chromosomally-encoded FliP-$M_{210}A$ variant ($M_{210}A$ gate, left) or wild type FliP (wild type gate, right). Wild type FliP and FliP-$M_{210}A$ were engineered to contain an internal HA tag positioned between residue 21 and 22 to allow immunodetection of FliP [29] (bottom panel). Both strains produced either a pTrc99a plasmid-encoded FlgD subunit variant in which residues 9-32 were replaced with two repeats of the six amino acid sequence Gly-Ser-Thr-Asn-Ala-Ser

976 ($FlgD_{short}$; top panel) or a pTrc99a plasmid-encoded wild type FlgD subunit ($FlgD_{wild}$

977 $_{type}$; middle panel). Proteins were separated by SDS (15%)-PAGE and analysed by

978 immunoblotting with anti-FlgD polyclonal antisera or anti-HA monoclonal antisera.

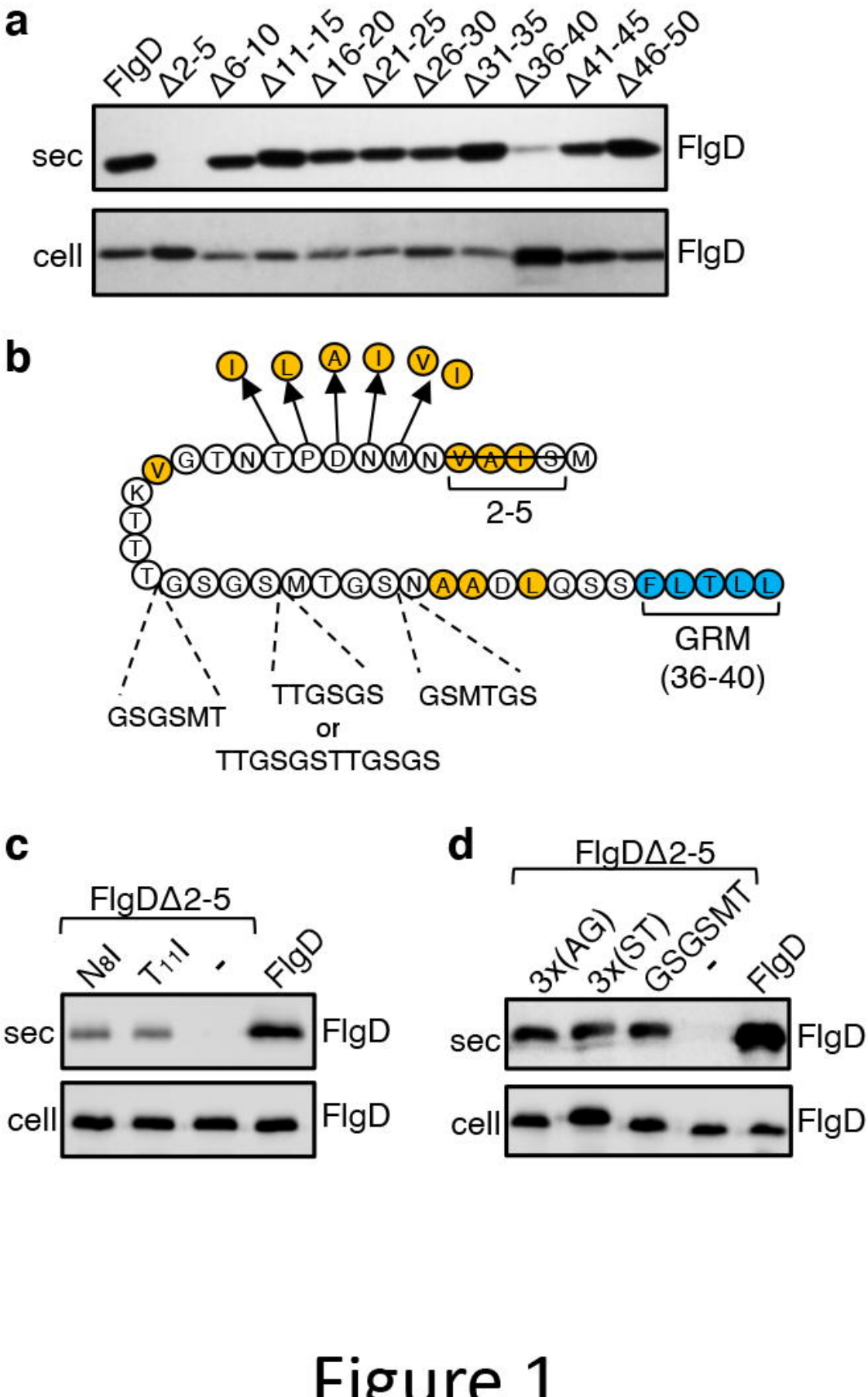
a
FlgD
Δ2-5
Δ6-10
Δ11-15
Δ16-20
Δ21-25
Δ26-30
Δ31-35
Δ36-40
Δ41-45
Δ46-50
sec
cell
FlgD
FlgD
b
I L A I V I
V G T N T P D N M N V A I S M
K T T T
T G S G S M T G S N A A D L Q S S F L T L L
2-5
GRM
(36-40)
GSGSMT
TTGSGS
or
TTGSGSTTGSGS
GSMTGS
c
FlgDΔ2-5
N8I
T11I
-
FlgD
sec
cell
FlgD
FlgD
d
FlgDΔ2-5
3x(AG)
3x(ST)
GSGSMT
-
FlgD
sec
cell
FlgD
FlgD

Figure 1

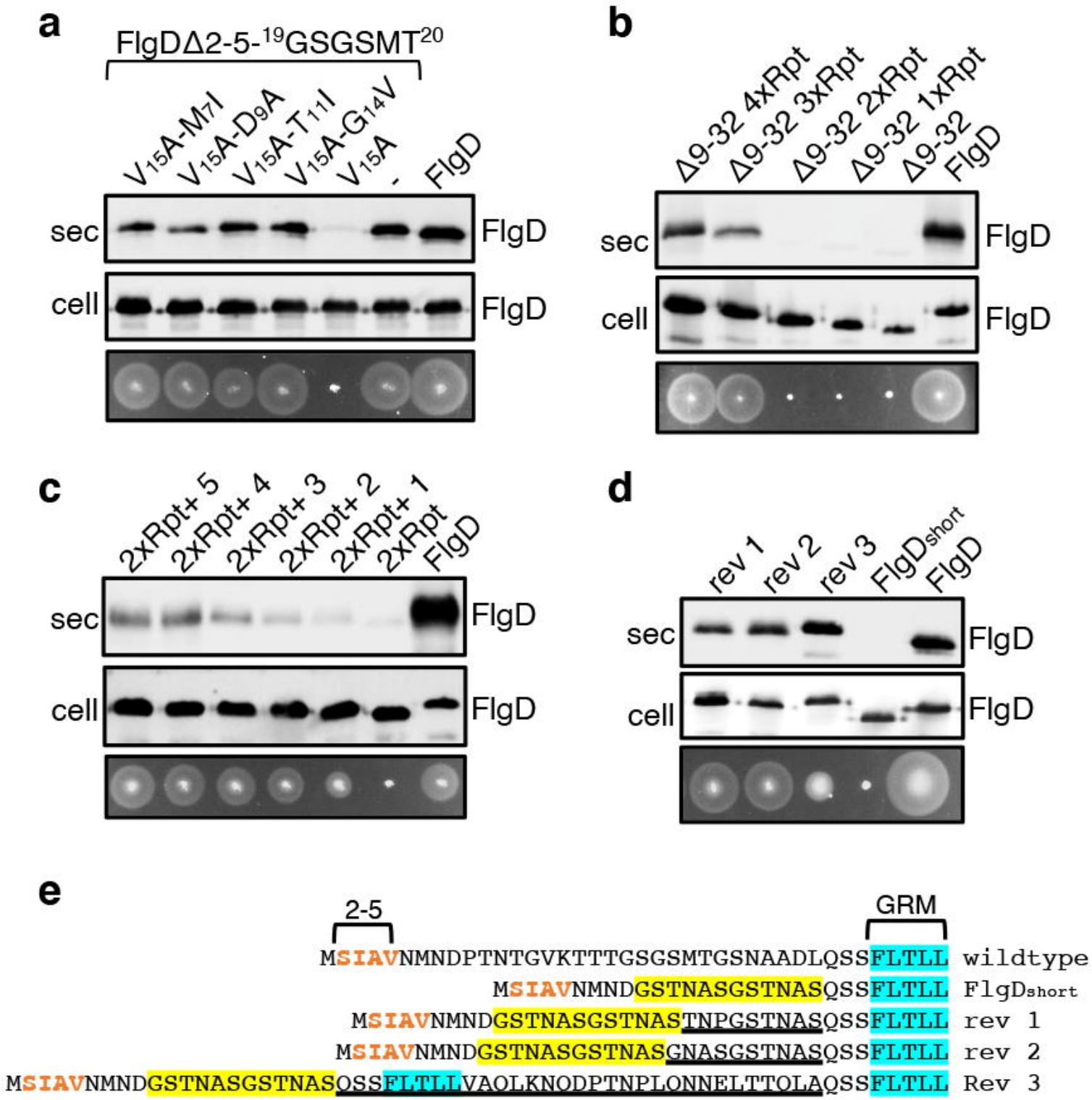
a
FlgDΔ2-5-19GSGSMT20
V15A-M7I
V15A-D9A
V15A-T11I
V15A-G14V
V15A
-
FlgD
sec
cell
FlgD
b
Δ9-32 4xRpt
Δ9-32 3xRpt
Δ9-32 2xRpt
Δ9-32 1xRpt
Δ9-32
FlgD
c
2xRpt+ 5
2xRpt+ 4
2xRpt+ 3
2xRpt+ 2
2xRpt+ 1
2xRpt
d
rev 1
rev 2
rev 3
FlgDshort
e
2-5
GRM
MSIAVNMNDPTNTGVKTTTGSGSMTGSNAADLQSSFLTLL wildtype
MSIAVNMNDGSTNASGSTNASQSSFLTLL FlgDshort
MSIAVNMNDGSTNASGSTNASTNPGSTNASQSSFLTLL rev 1
MSIAVNMNDGSTNASGSTNASGNASGSTNASQSSFLTLL rev 2
MSIAVNMNDGSTNASGSTNASQSSFLTLLVAQLKNQDPTNPLQNNELTTQLAQSSFLTLL Rev 3

Figure 2

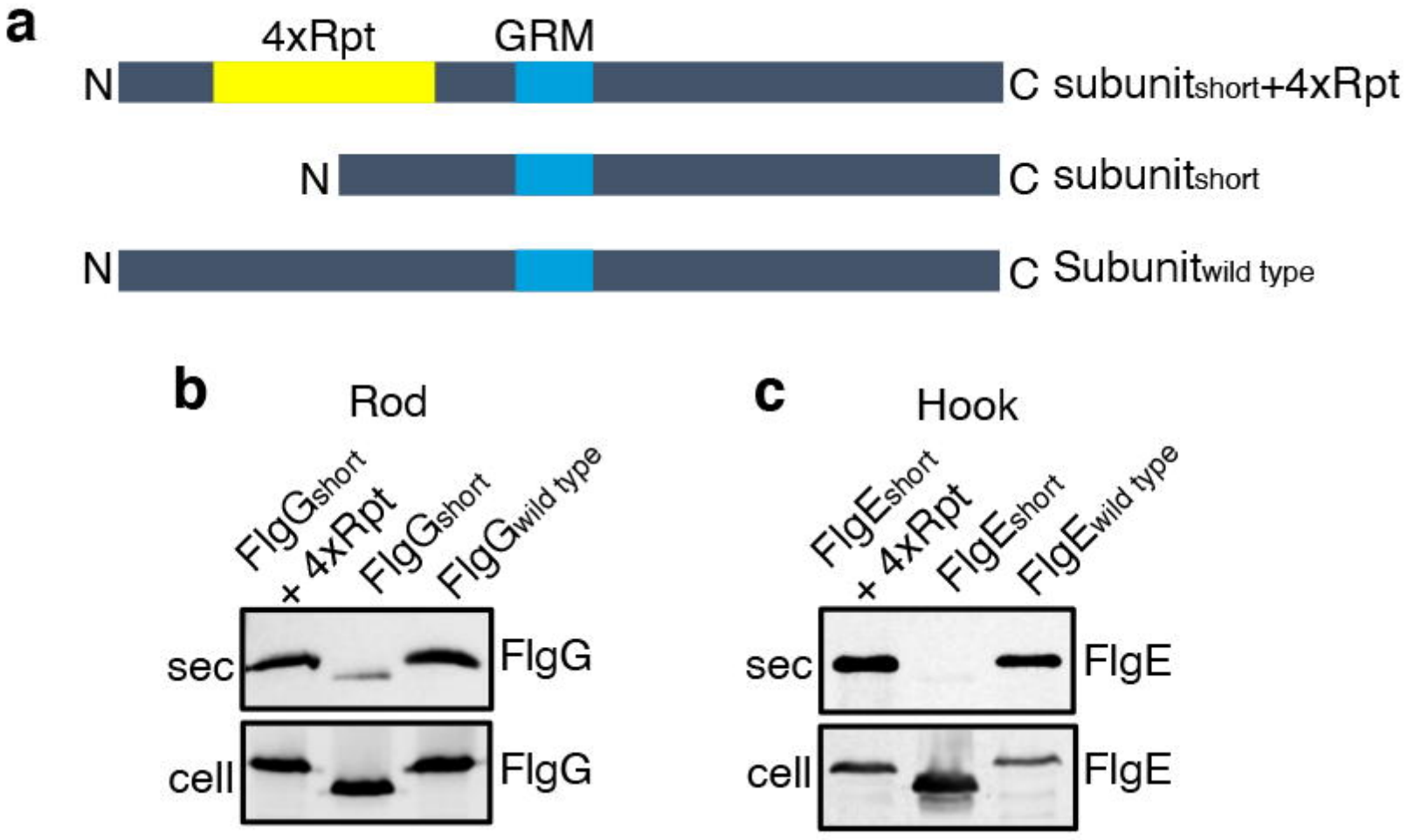
a
4xRpt
GRM
N
C subunitshort+4xRpt
N
C subunitshort
N
C Subunitwild type
b
Rod
FlgGshort + 4xRpt
FlgGshort
FlgGwild type
sec
FlgG
cell
FlgG
c
Hook
FlgEshort + 4xRpt
FlgEshort
FlgEwild type
sec
FlgE
cell
FlgE

Figure 3

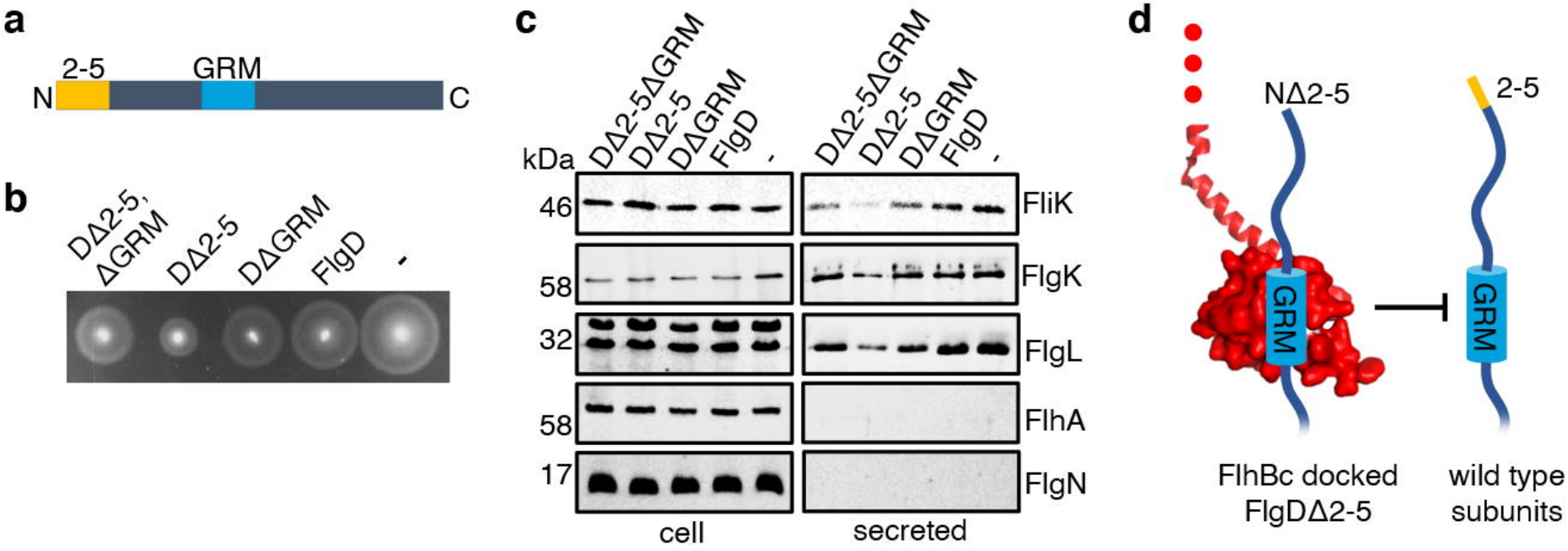
a
2-5
GRM
N
C
b
DΔ2-5, ΔGRM
DΔ2-5
DΔGRM
FlgD
-
c
kDa
DΔ2-5ΔGRM
DΔ2-5
DΔGRM
FlgD
-
DΔ2-5ΔGRM
DΔ2-5
DΔGRM
FlgD
-
46
58
32
58
17
FliK
FlgK
FlgL
FlhA
FlgN
cell
secreted
d
NΔ2-5
2-5
GRM
GRM
FlhBc docked
FlgDΔ2-5
wild type
subunits

Figure 4

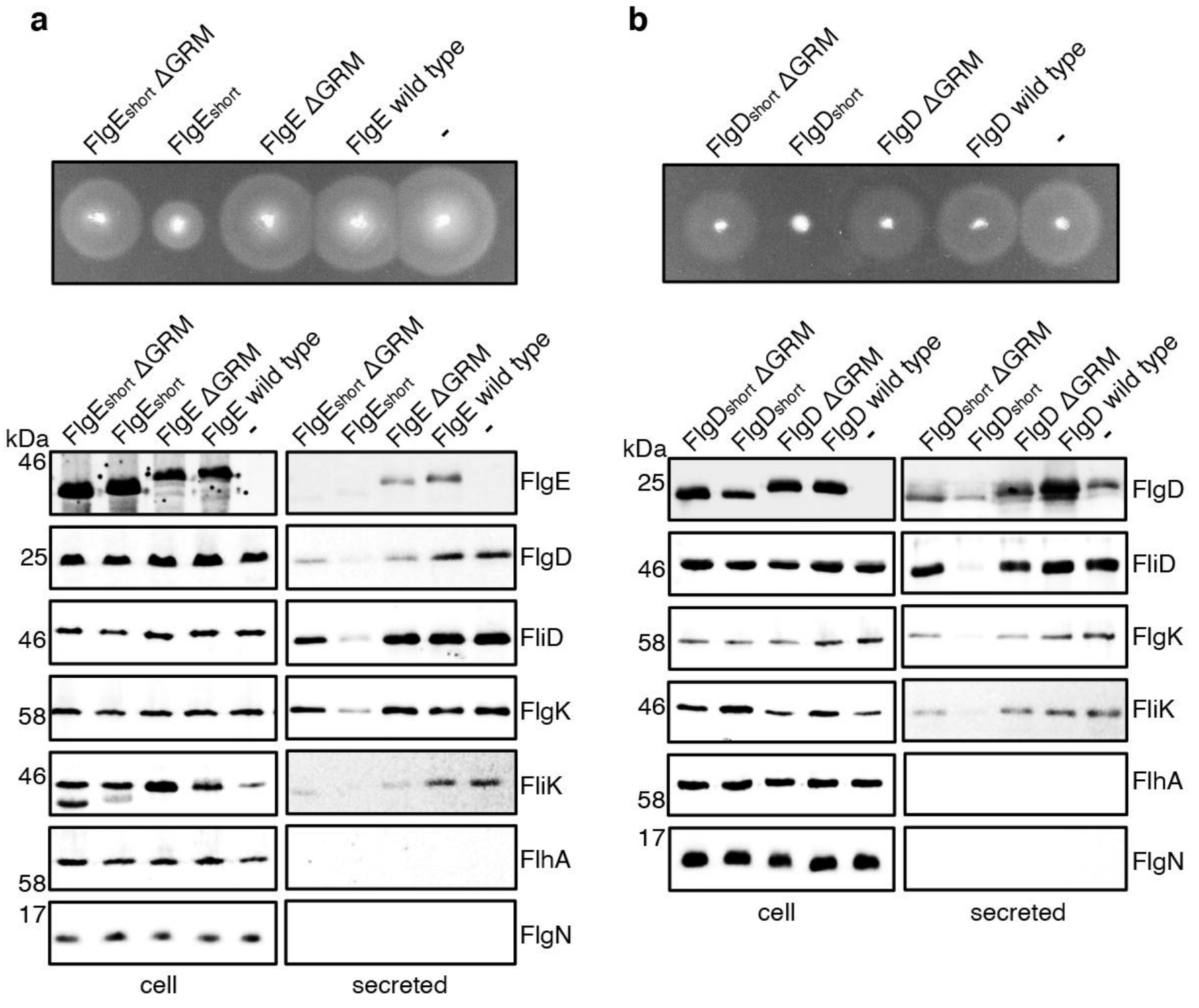
a
FlgEshort ΔGRM
FlgEshort
FlgE ΔGRM
FlgE wild type
-
kDa
46
25
46
58
46
58
17
FlgE
FlgD
FliD
FlgK
FliK
FlhA
FlgN
cell
secreted
b
FlgDshort ΔGRM
FlgDshort
FlgD ΔGRM
FlgD wild type
-
kDa
25
46
58
46
58
17
FlgD
FliD
FlgK
FliK
FlhA
FlgN
cell
secreted

Figure 5

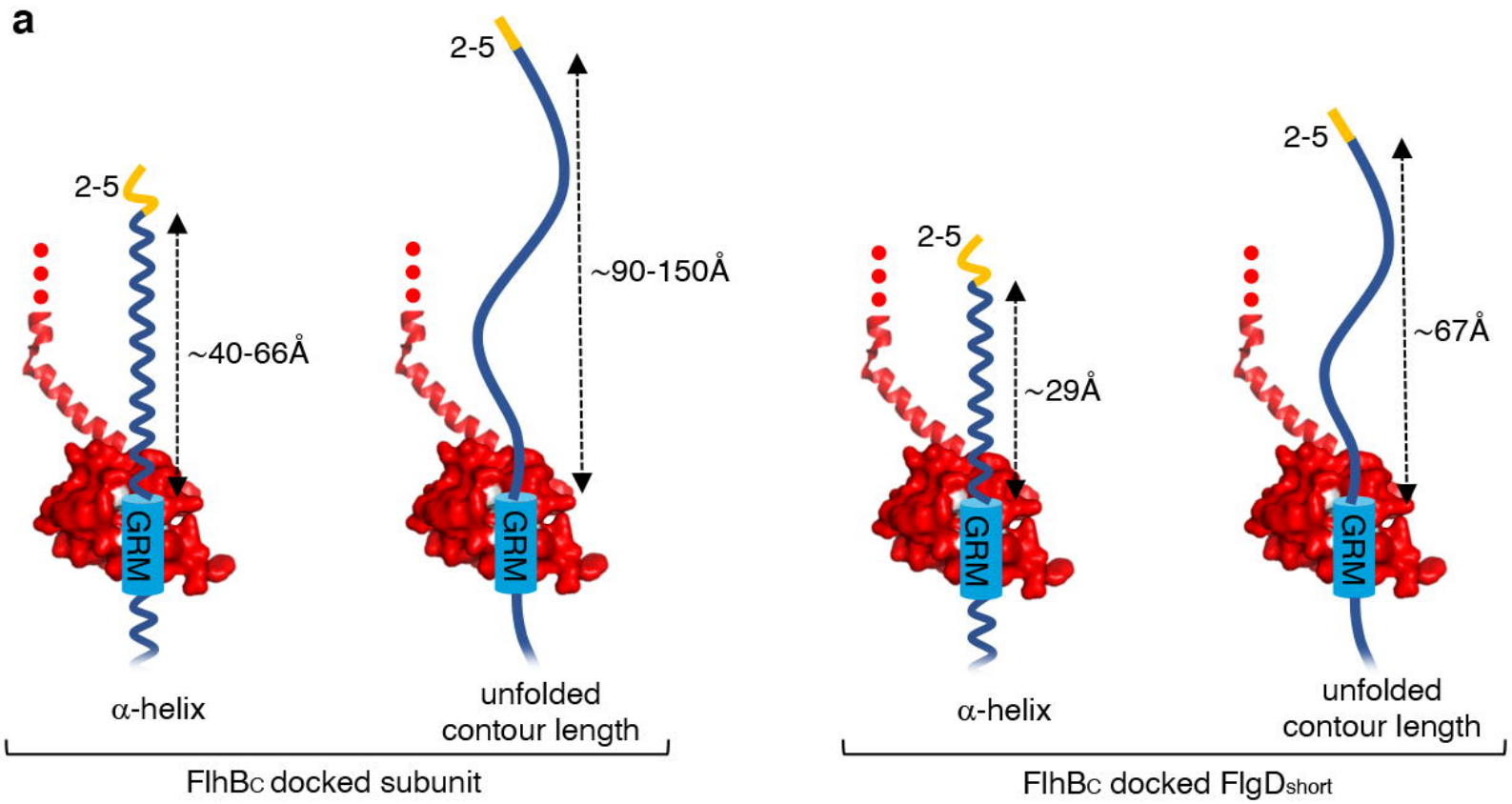
a
2-5
~40-66Å
GRM
2-5
~90-150Å
GRM
α-helix
unfolded
contour length
FlhBc docked subunit
2-5
~29Å
GRM
2-5
~67Å
GRM
α-helix
unfolded
contour length
FlhBc docked FlgDshort

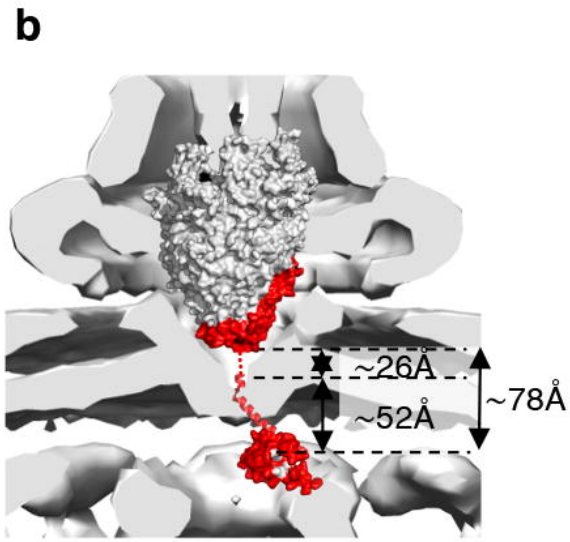
b
~26Å
~52Å
~78Å

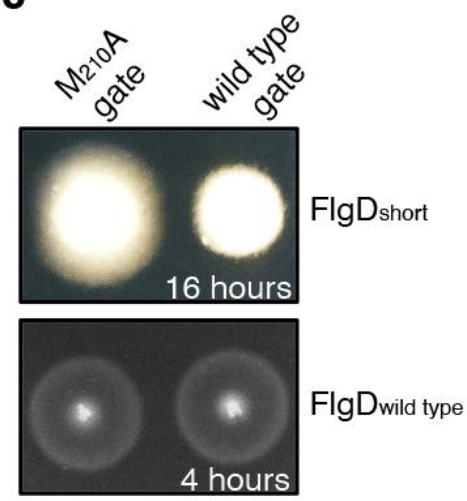
c
M210A
gate
wild type
gate
FlgDshort
16 hours
FlgDwild type
4 hours

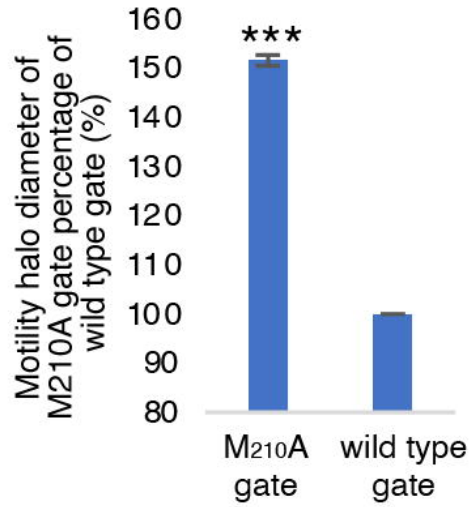
d
Motility halo diameter of
M210A gate percentage of
wild type gate (%)
160
150
140
130
120
110
100
90
80
***
M210A
gate
wild type
gate

Figure 6